

See discussions, stats, and author profiles for this publication at: <https://www.researchgate.net/publication/260483620>

Oxygen–Sulfur Exchange and the Gas–Phase Reactivity of Cobalt Sulfide Cluster Anions with Molecular Oxygen

ARTICLE *in* THE JOURNAL OF PHYSICAL CHEMISTRY A · MARCH 2014

Impact Factor: 2.69 · DOI: 10.1021/jp500837g · Source: PubMed

READS

41

4 AUTHORS, INCLUDING:



Zhixun Luo

Chinese Academy of Sciences

50 PUBLICATIONS 290 CITATIONS

SEE PROFILE



Sheng-Gui He

Chinese Academy of Sciences

153 PUBLICATIONS 2,491 CITATIONS

SEE PROFILE



Mao-Fa Ge

Chinese Academy of Sciences

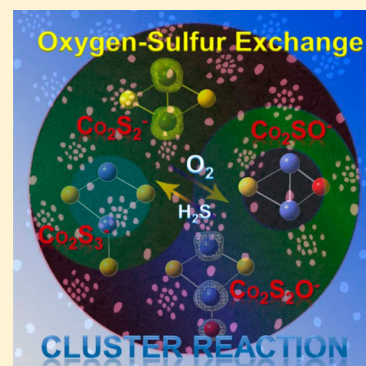
259 PUBLICATIONS 3,011 CITATIONS

SEE PROFILE

Oxygen–Sulfur Exchange and the Gas-Phase Reactivity of Cobalt Sulfide Cluster Anions with Molecular Oxygen

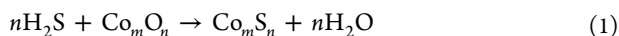
Mei-Ye Jia,^{†,‡} Zhixun Luo,^{*,†} Sheng-Gui He,^{*,†} and Mao-Fa Ge[†][†]Beijing National Laboratory for Molecular Sciences, State Key Laboratory for Structural Chemistry of Unstable and Stable Species, Institute of Chemistry, Chinese Academy of Sciences, Beijing 100190, China[‡]University of Chinese Academy of Sciences, Beijing 100049, China

ABSTRACT: We present here a study of gas-phase reactivity of cobalt sulfide cluster anions Co_mS_n^- with molecular oxygen. Nascent Co_mS_n^- clusters were prepared via a laser ablation source and reacted with oxygen in a fast flow reactor under thermal collision conditions. We chose $^{18}\text{O}_2$ in place of $^{16}\text{O}_2$ to avoid mass degeneration with sulfur, and a time-of-flight (TOF) mass spectrometer was used to detect the cluster distributions in the absence and presence of the reactant. It was found that oxygen–sulfur exchange occurs in the reactions for those with specific compositions $(\text{CoS})_n^-$ and $(\text{CoS})_n\text{S}^-$ ($n = 2-5$) according to a consistent pathway, “ $\text{Co}_m\text{S}_n^- + ^{18}\text{O}_2 \rightarrow \text{Co}_m\text{S}_{n-1}^{18}\text{O}^- + \text{S}^{18}\text{O}$ ”. Typically, for “ $\text{Co}_2\text{S}_2^- + ^{18}\text{O}_2$ ” we have calculated the reaction coordinates by employing the density functional theory (DFT), where both the oxygen–sulfur exchange and SO molecule release are thermodynamically and kinetically favorable. It is noteworthy that the reaction with molecular oxygen (triplet ground state) needs to overcome a spin excitation as well as a large O–O activation energy. This study sheds light on the activation of molecular oxygen by cobalt sulfides on one hand and also provides insight into the regeneration mechanism of cobalt oxides from the counterpart sulfides in the presence of oxygen gas on the other hand.



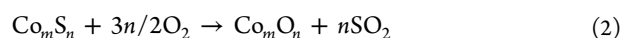
1. INTRODUCTION

Transition-metal sulfides are of significance in catalytic processes and biochemical systems.^{1–4} In general combination with molybdenum, cobalt sulfides are widely used as catalysts for industrial process such as hydrosulfurization implemented in large-scale refining.^{5–9} The best defined sulfides of cobalt exist in rare minerals, such as the rare mineral cattierite with a main stoichiometry CoS_2 .¹⁰ Besides, cobalt sulfides are produced in some industrial and chemical processes, typically in the adsorptive and catalytic removal of H_2S from waste gases in petroleum, gas, and metallurgical industries.¹¹ In these chemical processes, cobalt sulfides can be generated during the initial stages of H_2S interacting with cobalt oxide surfaces:^{12,13}



In this process of eq 1, the cobalt oxides function as reactants, also adsorbents and catalysts, leading to the production of cobalt sulfides and a conversion of H_2S into H_2O . To elucidate the molecular-level reaction mechanisms involved in the removal of H_2S , recently we have systematically studied the gas-phase reactions of transition-metal oxide cluster anions M_mO_n^- ($\text{M} = \text{V}, \text{Mn}, \text{Fe}, \text{Co}, \text{Ni}, \text{Cu}, \text{and Zn}$) and also cationic M_mO_n^+ with H_2S .^{13–17} It was found that, in addition to H_2S adsorption to form association products, another three types of reactions are evidenced (thermodynamically and kinetically favorable) in the reactor by producing HS , S , and H_2O , respectively. These studies including structures and reactivity of cobalt oxide clusters help provide insights into the mechanisms of H_2S transformation over metal oxide surfaces.

It is equally important to note that cobalt oxides can be regenerated from the cobalt sulfides at low temperatures in the presence of oxygen,^{11,18,19}



which indicates application potentials for recycled use via further H_2S adsorption. Such two reaction pathways demonstrate interesting oxygen–sulfur exchange process.²⁰ However, the detailed molecular-level mechanism for the regeneration of cobalt oxides from cobalt sulfides (i.e., oxygen–sulfur exchange) is still illusive to be further explored.

As is well-known, molecular oxygen is spin triplet in its ground state, and the two half-filled molecular orbitals are antibonding in nature, which means that the activation of molecular oxygen requires to fill the half-filled antibonding orbitals in $^3\text{O}_2$ and to reduce the multiplicity of the molecule from triplet to singlet. In this point, previous studies have demonstrated that spin accommodation determines the reactivity of metal cluster anions with oxygen.^{21,22} For example, Ag_n^- clusters with even numbers of Ag atoms (odd numbers of electrons) are much more reactive than their counterparts of odd atoms (even numbers of electrons); together with theoretical studies, it has been found that this behavior is correlated with the spin excitations needed to activate the O–O

Special Issue: A. W. Castleman, Jr. Festschrift

Received: January 24, 2014

Revised: February 18, 2014

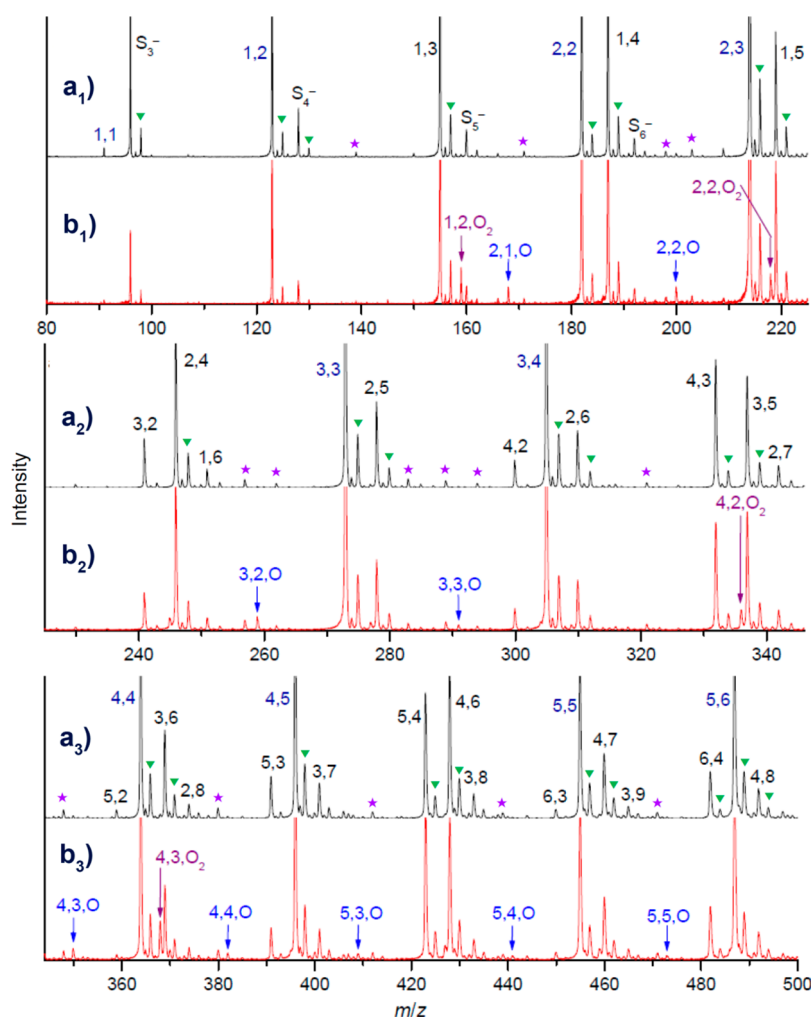


Figure 1. Time-of-flight mass spectra of Co_mS_n^- ($m = 1-5$) in the absence (a_1, a_2, a_3) and presence (b_1, b_2, b_3) of molecular oxygen $^{18}\text{O}_2$. Partial pressure of $^{18}\text{O}_2$ in the reactor is approximately 1.2 Pa for b_1-b_3 . Symbols m,n , m,n,O , and m,n,O_2 denote Co_mS_n^- , $\text{Co}_m\text{S}_n^{18}\text{O}^-$, and $\text{Co}_m\text{S}_n^{18}\text{O}_2^-$, respectively. In a_1-a_3 , the stars and triangles mark the minor peaks of $\text{Co}_m\text{S}_n^{16}\text{O}^-$ and $\text{Co}_m^{34}\text{S}_n^-$, respectively.

bond in molecular oxygen.²³ On the other hand, it is well-known that oxidative transformations of stable molecules on surfaces also often involve reactive oxygen species (ROS).²⁴⁻²⁹ Specifically, for condensed-phase reactions involving molecular oxygen, the O_2 molecule is considered to dissociate in the following scheme: O_2 (molecular oxygen) $\rightarrow \text{O}_2^{\bullet}$ (super-oxide) $\rightarrow \text{O}_2^{2-}$ (peroxide) $\rightarrow 2\text{O}^{\bullet}$ (mononuclear oxygen-centered radical) $\rightarrow 2\text{O}^{2-}$ (lattice oxygen), among which the O_2^{\bullet} , O_2^{2-} , and O^{\bullet} are ROS.³⁰ The chemical reactions toward oxygen are ubiquitous with important scientific issues involved.

In this study, we have presented an investigation into the reactions of cobalt sulfide cluster anions Co_mS_n^- with O_2 by a joint experimental and theoretical approach, that is, via time-of-flight (TOF) mass spectrometry and density functional theory (DFT) calculations. As results, the oxygen-sulfur exchange dominates the reactions of Co_mS_n^- ($n = 2-5$) according to a consistent pathway “ $\text{Co}_m\text{S}_n^- + ^{18}\text{O}_2 \rightarrow \text{Co}_m\text{S}_{n-1}^{18}\text{O}^- + \text{S}^{18}\text{O}$ ”. The regeneration of cobalt oxides (e.g., Co_2O_2) from the counterpart sulfides (e.g., Co_2S_2) simply in the presence of molecular oxygen suggests valuable cluster species for repeated use in H_2S pollution treatment. Also it is expected to validate an effective approach revealing such mechanistic details in condensed-phase reactions by studying their cluster reactivity under well-controlled gas-phase conditions.

2. EXPERIMENTAL AND THEORETICAL METHODS

2.1. Experimental Section. The experiments were conducted by a TOF mass spectrometer (TOF-MS) coupled with a laser ablation cluster source and a fast flow reactor.³¹ The Co_mS_n^- clusters were produced by laser ablation of a rotating and translating cobalt sulfide disk (Co/S mole ratio of 2:1) in the presence of a helium carrier gas with a backing pressure of 5 atm. A 532 nm (second harmonic of Nd^{3+} : yttrium aluminum garnet-YAG) laser was used, with an energy of 5–8 mJ/pulse and repetition rate of 10 Hz. The gas was controlled by a pulsed valve (General Valve, Series 9). To prevent residual water in the gas handling system from forming undesirable hydroxo species, the carrier gas He was passed through a 10 m long copper tube coil at low temperature ($T = 77$ K) before entering into the pulsed valve. Similar treatment was also applied in the use of the reaction gas (1% $^{18}\text{O}_2$ seeded in He) that was pulsed into the reactor 20 mm downstream from the exit of the narrow cluster formation channel by a second pulsed valve (General Valve, Series 9). The choice of $^{18}\text{O}_2$ as the reaction gas is based on a consideration to avoid the confusion and uncertainty of Co_mS_n^- clusters, as the mass number of $^{16}\text{O}_2$ is identical to that of a sulfur atom. With our method as presented previously,³² the instantaneous total gas pressure in the fast flow reactor was estimated to be around 220

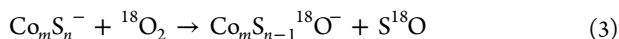
Pa at $T = 300$ K. The intracluster vibrations were likely equilibrated (cooled or heated, depending on the vibration temperature after exiting cluster formation channel with a supersonic expansion) to the bath gas temperature before reacting with the diluted $^{18}\text{O}_2$. It is anticipated that the bath gas has the same temperature as the wall of the reactor,³³ and actually our recent experiments indicated that the cluster vibrational temperature in the reactor was close to 300 K.^{34,35} After sufficient reaction in the fast flow tube reactor, the reactant and product ions were skimmed into the TOF-MS vacuum system for mass and abundance measurements. The uncertainty of the relative ion signals is no more than $\sim 15\%$ and mass resolution ($M/\Delta M$) is at 400–500 with current experimental setup. More details of the experiments can be found in our previous work.³⁶

2.2. Computational Details. DFT calculations with Gaussian 09 program³⁷ were performed to investigate the reaction mechanisms of “ $\text{Co}_2\text{S}_2^- + \text{O}_2$ ”. The hybrid B3LYP functional^{38,39} with the 6-311+G(d) basis set⁴⁰ was used in this study. The choice of B3LYP method with moderate computational cost has been tested to provide reasonable results for cobalt sulfides.^{41,42} Geometry optimizations of all the reaction intermediates and transition states on the potential energy surfaces were carried out with full relaxation of all atoms. Vibrational frequency calculations were carried out to ensure that the reaction intermediates and transition state species have zero and one imaginary frequency, respectively. The DFT-calculated energies reported in this study are corrected ($\Delta H_{0\text{K}}$) on the basis of zero-point vibrational energies (ZPE) and the relative Gibbs free energies ($\Delta G_{298\text{K}}$) under a temperature of 298.15 K and pressure of 1.0 atm. Structures and vibrational frequencies for all of the optimized structures are available on request.

3. RESULTS AND DISCUSSION

Figure 1 plots a typical TOF mass spectrum result before (parts a₁–a₃) and after (parts b₁–b₃) reacting with $^{18}\text{O}_2$ at a partial pressure of about 1.2 Pa in the reactor. Among the nascent spectrum (Figure 1a, parts a₁–a₃), besides a few peaks due to elemental sulfur, notable Co_mS_n^- series dominate the observed cluster species, and mostly the atom numbers of n are larger than m . In particular, $(\text{CoS})_m^-$ and $(\text{CoS})_m\text{S}^-$ series display the maximal intensities. The existence of $(\text{CoS})_m\text{S}^-$, similar to $\text{M}^+(\text{MX})_n$, resembles the “F-center” localization in bulk alkali metal halide crystals,^{43–49} but there is difference as the interaction of excess electrons plays an important role in the outcome of cobalt sulfide clusters. Considering cobalt has an electronic configuration of $1s^2 2s^2 2p^6 3s^2 3p^6 3d^7 4s^2$ and its metal oxidation state generally displays +2 or +3, it is reasonable to form such stable species as Co_2S_2 and Co_2S_3 , etc.

Ion molecule reactions often generate simple addition products,^{50,51} and such products are seen in our experiments, e.g., $\text{Co}_2\text{S}_2^{18}\text{O}_2^-$, $\text{Co}_4\text{S}_3^{18}\text{O}_2^-$, etc. However, besides this simple addition reaction pathway, several product peaks assigned to $\text{Co}_m\text{S}_{n-1}^{18}\text{O}^-$ were observed, especially for those clusters with specific compositions $(\text{CoS})_n^-$ and $(\text{CoS})_n\text{S}^-$ ($n = 2-5$), suggesting an interesting oxygen–sulfur exchange reaction channel, expressed as



To further illustrate this interesting reactivity, Figure 2 displays an enlarged area for 167–183 amu, where the relative

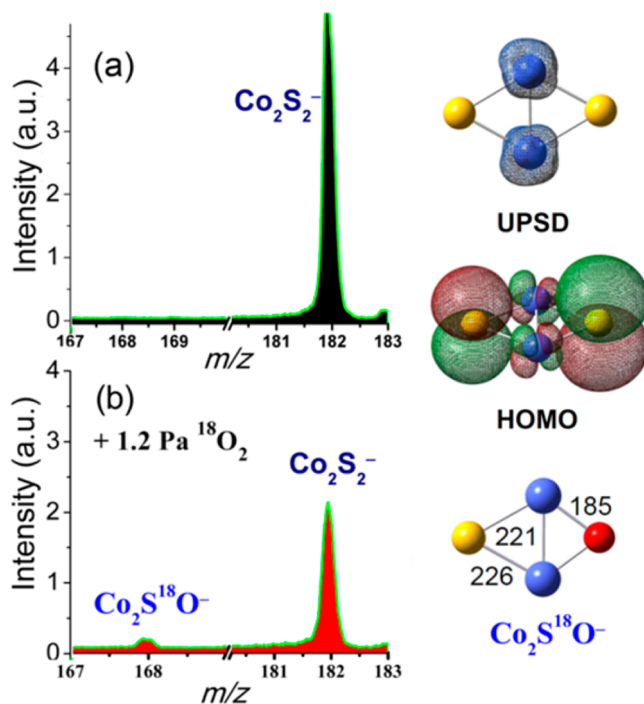
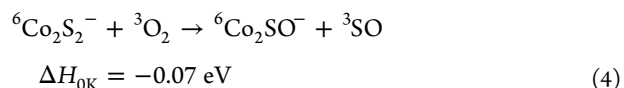


Figure 2. Enlarged area in Figure 1a,b, displaying the relative intensity in the reaction. The insets on the right display the chemical structures of Co_2S_2^- and $\text{Co}_2\text{S}^{18}\text{O}^-$. The unpaired spin density distribution (UPSD) and the highest occupied molecular orbital (HOMO) for Co_2S_2^- are also displayed.

intensity of Co_2S_2^- is apparently reduced when reacting with $^{18}\text{O}_2$, together with a production of $\text{Co}_2\text{S}^{18}\text{O}^-$. This finding leads to our in-depth study on the cluster reactivity of “ $\text{Co}_2\text{S}_2^- + \text{O}_2$ ” as discussed below. It is worth mentioning that the total intensity of the product $\text{Co}_2\text{S}^{18}\text{O}^-$ and remaining Co_2S_2^- (even including $\text{Co}_2\text{S}_2^{18}\text{O}_2^-$ as seen in Figure 1) is still not as large as the nascent Co_2S_2^- , indicating that unreactive scattering is involved.^{52,53}

To elucidate the experimental results that oxygen–sulfur exchange reactions can readily take place under thermal collision conditions, DFT calculations were emphasized on the following reaction:



The superscripts indicate the spin multiplicities for the reactant and product species, and the $\Delta H_{0\text{K}}$ value refers to the DFT calculated enthalpy. The DFT calculated reaction coordinates for “ $\text{Co}_2\text{S}_2^- + \text{O}_2$ ” are shown in Figure 3 where the energies are directly marked out. Upon the approach of O_2 to Co_2S_2^- , the Co–O₂ bond forms immediately along with an elongation of the O–O bond from 121 to 132 pm, and this process “ $\text{Co}_2\text{S}_2^- + \text{O}_2 \rightarrow \text{Co}_2\text{S}_2\text{O}_2^-$ (I_1)” aims at a heat release of 1.46 eV ($\Delta H_{0\text{K}}$), which is high enough to provide the energy needed for the bond cleavage of O–O. The O–O distance gradually increases (132 pm \rightarrow 142 pm \rightarrow 147 pm \rightarrow 182 pm), and the OS moiety is formed in the most stable intermediate I_3 ($I_1 \rightarrow \text{TS}_{1/2} \rightarrow I_2 \rightarrow \text{TS}_{2/3} \rightarrow I_3$). It is noteworthy that the O_2 moieties in I_1 and I_2 can be denoted as $\text{O}_2^{\bullet -}$ (superoxide) and O_2^{2-} (peroxide), respectively, on the basis of the analysis of the unpaired spin densities on O atoms. The energy released during the formation of I_3 assists in the formation of Co–O bond in

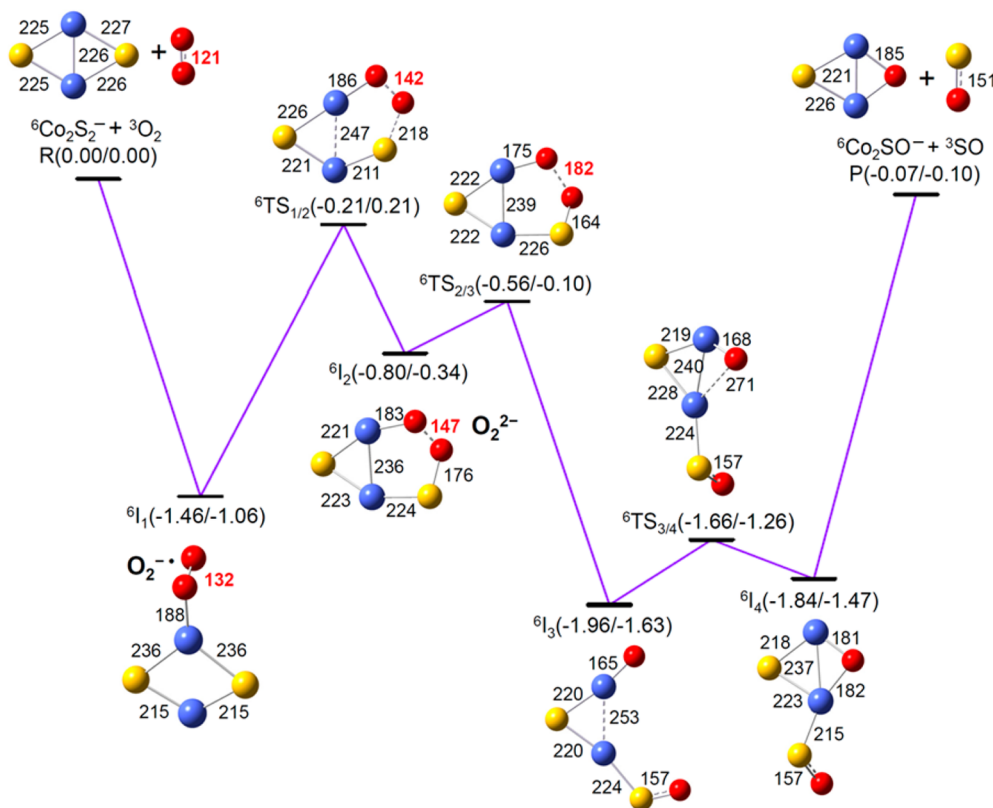


Figure 3. B3LYP/6-311+G(d) calculated oxygen–sulfur exchange reaction pathway for “ ${}^6\text{Co}_2\text{S}_2^- + {}^3\text{O}_2$ ”. The reaction intermediates and transition states are denoted as 6I_n and ${}^6\text{TS}_{n1/n2}$, respectively. The superscripts 6 and 3 indicate the spin multiplicities for the reaction species from the very beginning to the end of the reaction. The relative energies of $\Delta H_{0\text{K}}$ and $\Delta G_{298\text{K}}$ (in electronvolts) with respect to the separated reactants Co_2S_2^- and O_2 are provided in parentheses. Bond lengths are given in picometers.

intermediate I_4 ($I_3 \rightarrow \text{TS}_{3/4} \rightarrow I_4$) and the generation of products Co_2SO^- and SO . In addition, the transition states $\text{TS}_{1/2}$, $\text{TS}_{2/3}$, and $\text{TS}_{3/4}$ are lower in energy than the separated reactants Co_2S_2^- and O_2 , allowing the oxygen–sulfur exchange reaction to be both kinetically and thermodynamically favorable. The DFT result is consistent with the experimental observation of the generation of Co_2SO^- (Figure 1b₁ and Figure 2).

It is noteworthy that intermediates I_3 and I_4 are much lower in energy than the products $\text{Co}_2\text{SO}^- + \text{SO}$ and the reactants $\text{Co}_2\text{S}_2^- + \text{O}_2$. Given that those reaction intermediates carrying not only the binding energy between Co_2S_2^- and O_2 but also the center-of-mass kinetic energy as well as the vibrational energy of the reactants can be stabilized by collisions (rate $\sim 10^7 \text{ s}^{-1}$)³⁵ with the helium bath gas in the reactor, they are possibly observed in the experiment.¹⁷ This is also consistent with the experimental observation of the product peak labeled as “2,2, O_2 ” in Figure 1b₁, which is assigned to the aforementioned intermediates I_3 and I_4 (more likely I_3).

Intensity changes of nascent Co_mS_n^- clusters and related products are associated with their reaction rates. With care taken during the repeated experiments, we have examined the intensities of several Co_mS_n^- species before and after reacting with ${}^{18}\text{O}_2$. The pseudo-first-order rate constant (k_1) in the fast flow reactor can be estimated by using the following equation:^{32,52}

$$k_1 = -\frac{\ln(I/I_0)}{\rho \times \Delta t} \quad (5)$$

Here, the ratio I/I_0 is the proportion of unreacted clusters after the cluster interaction with reactant gas that has molecular density of ρ in the reactor for reaction time of Δt . The estimated rate constants for Co_mS_n^- with ${}^{18}\text{O}_2$ by using the data in Figure 1 are listed in Table 1. It is shown that Co_2S_2^- is the most reactive cluster toward the oxygen molecule, up to $4.1 \times 10^{-11} \text{ cm}^3 \text{ molecule}^{-1} \text{ s}^{-1}$.

Table 1. Pseudo-First-Order Rate Constants ($k_1/\text{cm}^3 \text{ molecule}^{-1} \text{ s}^{-1}$) for Reactions of Co_mS_n^- with ${}^{18}\text{O}_2$

Co_mS_n^-	$10^{12} k_1$	Co_mS_n^-	$10^{12} k_1$
CoS_2^-	23	Co_4S_4^-	10
Co_2S_2^-	41	Co_4S_5^-	6
Co_2S_3^-	8	Co_5S_4^-	5
Co_3S_3^-	7	Co_5S_5^-	4
Co_3S_4^-	6	Co_5S_6^-	3

Besides these typical examples, many other cobalt sulfide clusters also react with molecular oxygen although their reactivities and rate constants differ from each other. Previously, gas-phase investigations have concluded that the reactivity of atomic clusters can be very sensitive to the composition, size, charge, and electronic state details, hence allowing some of them to be more reactive than their counterparts even in the same serial.^{53–55} For example, through the studies of Al clusters reacting with D_2O ,⁵⁶ it was established that size-selective reactivity of clusters could be caused by complementary active sites that refer to two locations on the cluster surface where one location behaves like a Lewis acid (accepting the electrons from

the oxygen) and an adjacent location behaves as a Lewis base (donating electrons to the hydrogen).⁵⁷ Among others, recently in the reaction pathways of VO_4^- with H_2S , the oxygen–sulfur exchange involving peroxide unit in VO_4^- has been unambiguously demonstrated, where all of the four O atoms in VO_4^- can be substituted by S atoms to form VS_4^- .¹⁶ Here in the present work, the peroxide moiety O_2^{2-} derived from the dissociation of O_2 molecule over Co_2S_2^- cluster ($\text{I}_1 \rightarrow \text{TS}_{1/2} \rightarrow \text{I}_2$ in Figure 3) is proposed to be responsible for the oxygen–sulfur exchange reaction; and it may not always be necessary for the molecular oxygen (O_2) to completely dissociate into oxygen-centered radical (O^\bullet) or lattice oxygen (O^{2-}) in leading to the oxygen–sulfur exchange reactions.

It is worth mentioning that many investigations have been conducted to understand mechanistic details involved with removal of poisonous H_2S ,^{20,24} including our recent studies of the cluster reactions between M_mO_n^- ($\text{M} = \text{Fe}, \text{Co}, \text{Ni}, \text{Cu}$, and Zn) and hydrogen sulfide.¹³ Owing to the contribution of peroxide (O_2^{2-}), oxygen–sulfur exchange found in the reactivity of cobalt sulfides enables regeneration of certain cobalt oxides from their related sulfides and hence displays reutilization potentials. Figure 4 presents such an experimental

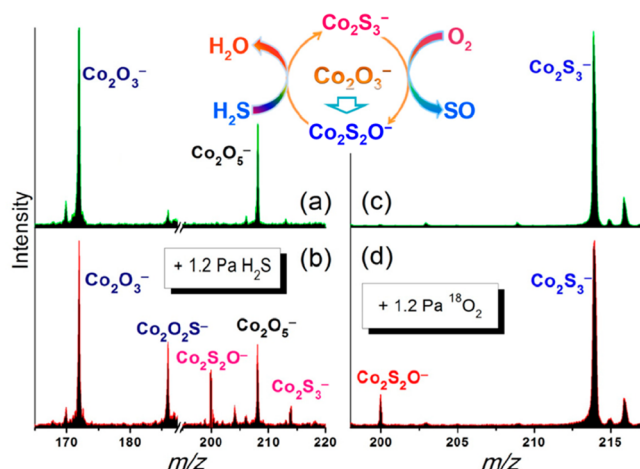


Figure 4. Comparison of the reactions of “ $\text{Co}_2^{18}\text{O}_3^- + \text{H}_2\text{S}$ ” (a/b) with “ $\text{Co}_2\text{S}_3^- + {}^{18}\text{O}_2$ ” (c/d). Intensities of clusters Co_2O_5^- in (a); $\text{Co}_2\text{S}_2\text{O}^-$, Co_2O_5^- , and Co_2S_3^- in (b); and $\text{Co}_2\text{S}_2\text{O}^-$ in (d) are scaled by a factor of 3. The data in (a) and (b) are adapted from ref 13.

conception, where Co_2O_3^- reacts with H_2S leading to $\text{Co}_2\text{S}_2\text{O}^-$, which can further react with H_2S to form Co_2S_3^- ; on the other hand, Co_2S_3^- reacts with oxygen and produces $\text{Co}_2\text{S}_2\text{O}^-$, resulting in recycling reaction pathways.

4. CONCLUSION

Reactivity of cobalt sulfide cluster anions Co_mS_n^- with ${}^{18}\text{O}_2$ under thermal collision conditions was studied by mass spectrometry and density functional theory calculations. The oxygen–sulfur exchange to generate oxygen-containing cobalt sulfide clusters $\text{Co}_m\text{S}_{n-1}{}^{18}\text{O}^-$ was observed in the reactions of clusters with specific compositions $(\text{CoS})_n^-$ and $(\text{CoS})_n\text{S}^-$ ($n = 2-5$). Typically, for “ $\text{Co}_2\text{S}_2^- + {}^{18}\text{O}_2$ ” we have calculated the reaction coordinates and found consistent results with the experimental observations. Through the joint experimental and theoretical studies, we demonstrate the determining role of peroxide moiety O_2^{2-} for the O–O bond activation in the molecular oxygen reactions “ $\text{Co}_m\text{S}_n^- + {}^{18}\text{O}_2$ ”. This finding of

O–O bond cleavage in the gas-phase reactions of cobalt sulfides with ${}^{18}\text{O}_2$ enables the regeneration of certain cobalt oxides from their related sulfides simply by reacting with oxygen.

AUTHOR INFORMATION

Corresponding Authors

*Z. Luo: e-mail, zxlue@iccas.ac.cn; tel, +86-10-82617312; fax, +86-10-82616517.

*S.-G. He: e-mail, shengguihe@iccas.ac.cn; tel, +86-10-62536990; fax, +86-10-62559373.

Notes

The authors declare no competing financial interest.

ACKNOWLEDGMENTS

This work was supported by Chinese Academy of Sciences (Knowledge Innovation Program No. KJCX2-EW-H01), the National Natural Science Foundation of China (No. 21325314), and the 973 Program (Nos. 2011CB932302 and 2013CB834603).

REFERENCES

- (1) Stiefel, E. I.; Matsumoto, K. *Transition Metal Sulfur Chemistry, Biological and Industrial Significance*; American Chemical Society: Washington, DC, 1997.
- (2) Chianelli, R. R.; Berhault, G.; Torres, B. Unsupported Transition Metal Sulfide Catalysts: 100 Years of Science and Application. *Catal. Today* **2009**, *147*, 275–286.
- (3) Kretschmar, I.; Schröder, D.; Schwarz, H. Experimental and Theoretical Studies of Vanadium Sulfide Cation. *J. Phys. Chem. A* **1998**, *102*, 10060–10073.
- (4) Dance, I. Understanding Structure and Reactivity of New Fundamental Inorganic Molecules: Metal Sulfides, Metalloporphyrins, and Nitrogenase. *Chem. Commun.* **1998**, 523–530.
- (5) Wentreck, P. R.; Wise, H. Hydrodesulfurization Activity and Defect Structure of Cobalt-Molybdenum Sulfide Catalyst. *Abstr. Pap. Am. Chem. Soc.* **1977**, *173*, 35.
- (6) Okamoto, Y.; Nagata, K.; Adachi, T.; Imanaka, T.; Inamura, K.; Takyu, T. Preparation and Characterization of Highly Dispersed Cobalt Oxide and Sulfide Catalysts Supported on SiO_2 . *J. Phys. Chem.* **1991**, *95*, 310–319.
- (7) Minato, Y.; Aoki, K.; Shirai, M.; Arai, M. Cobalt-Based Catalysts Prepared by a Sol-Gel Method for Thiophene Hydrodesulfurization. *Appl. Catal., A* **2001**, *209*, 79–84.
- (8) Ooi, S.; Zhang, H. B.; Hinode, H. The Hydrodesulfurization Activity and Characterization of Cobalt Chevrel Phase Sulfides. *React. Kinet. Catal. Lett.* **2004**, *82*, 89–95.
- (9) Tran, P. D.; Chiam, S. Y.; Boix, P. P.; Ren, Y.; Pramana, S. S.; Fize, J.; Artero, V.; Barber, J. Novel Cobalt/Nickel-Tungsten-Sulfide Catalysts for Electrocatalytic Hydrogen Generation from Water. *Energy Environ. Sci.* **2013**, *6*, 2452–2459.
- (10) Vaughan, D. J.; Rosso, K. M. Chemical Bonding in Sulfide Minerals. *Rev. Mineral. Geochem.* **2006**, *61*, 231–264.
- (11) Wieckowska, J. Catalytic and Adsorptive Desulfurization of Gases. *Catal. Today* **1995**, *24*, 405–465.
- (12) Yasyerli, S. Cerium–Manganese Mixed Oxides for High Temperature H_2S Removal and Activity Comparisons with V–Mn, Zn–Mn, Fe–Mn Sorbents. *Chem. Eng. Process* **2008**, *47*, 577–584.
- (13) Jia, M.-Y.; Ding, X.-L.; He, S.-G.; Ge, M.-F. Experimental and Theoretical Study of the Reactions between MO_2^- ($\text{M} = \text{Fe}, \text{Co}, \text{Ni}, \text{Cu}$, and Zn) Cluster Anions and Hydrogen Sulfide. *J. Phys. Chem. A* **2013**, *117*, 8377–8387.
- (14) Jia, M.-Y.; Xu, B.; Ding, X.-L.; He, S.-G.; Ge, M.-F. Experimental and Theoretical Study of the Reactions between Manganese Oxide Cluster Anions and Hydrogen Sulfide. *J. Phys. Chem. C* **2012**, *116*, 24184–24192.

- (15) Jia, M.-Y.; Xu, B.; Ding, X.-L.; Zhao, Y.-X.; He, S.-G.; Ge, M.-F. Experimental and Theoretical Study of the Reactions between Vanadium Oxide Cluster Cations and Hydrogen Sulfide. *J. Phys. Chem. C* **2012**, *116*, 9043–9048.
- (16) Jia, M.-Y.; Xu, B.; Deng, K.; He, S.-G.; Ge, M.-F. Consecutive Oxygen-for-Sulfur Exchange Reactions between Vanadium Oxide Cluster Anions and Hydrogen Sulfide. *J. Phys. Chem. A* **2014**, DOI: 10.1021/jp411961q.
- (17) Jia, M.-Y.; He, S.-G.; Ge, M.-F. Experimental and Theoretical Study of the Reactions between Manganese Oxide Cluster Cations and Hydrogen Sulfide. *Chin. J. Chem. Phys.* **2013**, *26*, 679–686.
- (18) Yoshimura, Y.; Matsubayashi, N.; Yokokawa, H.; Sato, T.; Shimada, H.; Nishijima, A. Temperature-Programmed Oxidation of Sulfided Cobalt-Molybdate Alumina Catalysts. *Ind. Eng. Chem. Res.* **1991**, *30*, 1092–1099.
- (19) Castner, D. G.; Watson, P. R. X-Ray Absorption Spectroscopy and X-Ray Photoelectron Spectroscopy Studies of Cobalt Catalysts. 3. Sulfidation Properties in Hydrogen Sulfide/Hydrogen. *J. Phys. Chem.* **1991**, *95*, 6617–6623.
- (20) Groenewold, G. S.; Hodges, B. D. M.; Scott, J. R.; Gianotto, A. K.; Appelhans, A. D.; Kessinger, G. F.; Wright, J. B. Oxygen-for-Sulfur Exchange in the Gas Phase: Reactions of Al and Si Oxyanions with H_2S . *J. Phys. Chem. A* **2001**, *105*, 4059–4064.
- (21) Reber, A. C.; Khanna, S. N.; Roach, P. J.; Woodward, W. H.; Castleman, A. W., Jr. Spin Accommodation and Reactivity of Aluminum Based Clusters with O_2 . *J. Am. Chem. Soc.* **2007**, *129*, 16098–16101.
- (22) Burgert, R.; Schnöckel, H.; Grubisic, A.; Li, X.; Stokes, S. T.; Bowen, K. H.; Ganteför, G. F.; Kiran, B.; Jena, P. Spin Conservation Accounts for Aluminum Cluster Anion Reactivity Pattern with O_2 . *Science* **2008**, *319*, 438–442.
- (23) Luo, Z.; Gamboa, G. U.; Smith, J. C.; Reber, A. C.; Reveles, J. U.; Khanna, S. N.; Castleman, A. W., Jr. Spin Accommodation and Reactivity of Silver Clusters with Oxygen: The Enhanced Stability of Ag_{13}^- . *J. Am. Chem. Soc.* **2012**, *134*, 18973–18978.
- (24) Whetten, R. L.; Cox, D. M.; Trevor, D. J.; Kaldor, A. Free Iron Clusters React Readily with O_2 and H_2S but Are Inert toward Methane. *J. Phys. Chem.* **1985**, *89*, 566–569.
- (25) Shi, Y.; Zhang, N.; Gao, Z.; Kong, F.; Zhu, Q. The Formation, Photodissociation, and Bond Structure of Cobalt–Sulfur Cluster Ions. *J. Chem. Phys.* **1994**, *101*, 9528–9533.
- (26) He, S.-G.; Xie, Y.; Guo, Y.; Bernstein, E. R. Formation, Detection, and Stability Studies of Neutral Vanadium Sulfide Clusters. *J. Chem. Phys.* **2007**, *126*, 194315.
- (27) Yin, S.; Wang, Z.; Bernstein, E. R. O-Atom Transport Catalysis by Neutral Manganese Oxide Clusters in the Gas Phase: Reactions with CO, C_2H_4 , NO_2 , and O_2 . *J. Chem. Phys.* **2013**, *139*, 4819059.
- (28) Kapiloff, E.; Ervin, K. M. Reactions of Cobalt Cluster Anions with Oxygen, Nitrogen, and Carbon Monoxide. *J. Phys. Chem. A* **1997**, *101*, 8460–8469.
- (29) Che, M.; Tench, A. Characterization and Reactivity of Mononuclear Oxygen Species on Oxide Surfaces. *J. Adv. Catal.* **1982**, *31*, 77–78.
- (30) Chiavarino, B.; Crestoni, M. E.; Fornarini, S. Gas-Phase Dioxigen Activation by Binuclear Manganese Clusters. *Chem.—Eur. J.* **2002**, *8*, 2740–2746.
- (31) Geusic, M. E.; Morse, M. D.; O'Brien, S. C.; Smalley, R. E. Surface Reactions of Metal Clusters I: The Fast Flow Cluster Reactor. *Rev. Sci. Instrum.* **1985**, *56*, 2123–2130.
- (32) Xue, W.; Wang, Z.-C.; He, S.-G.; Xie, Y.; Bernstein, E. R. Experimental and Theoretical Study of the Reactions between Small Neutral Iron Oxide Clusters and Carbon Monoxide. *J. Am. Chem. Soc.* **2008**, *130*, 15879–15888.
- (33) Wu, X.-N.; Xu, B.; Meng, J.-H.; He, S.-G. C-H Bond Activation by Nanosized Scandium Oxide Clusters in Gas-Phase. *Int. J. Mass Spectrom.* **2012**, *310*, 57–64.
- (34) Ding, X.-L.; Zhao, Y.-X.; Wu, X.-N.; Wang, Z.-C.; Ma, J.-B.; He, S.-G. Hydrogen-Atom Abstraction from Methane by Stoichiometric Vanadium-Silicon Heteronuclear Oxide Cluster Cations. *Chem.—Eur. J.* **2010**, *16*, 11463–11470.
- (35) Wu, X.-N.; Ma, J.-B.; Xu, B.; Zhao, Y.-X.; Ding, X.-L.; He, S.-G. Collision-Induced Dissociation and Density Functional Theory Studies of CO Adsorption over Zirconium Oxide Cluster Ions: Oxidative and Nonoxidative Adsorption. *J. Phys. Chem. A* **2011**, *115*, 5238–5246.
- (36) Xue, W.; Yin, S.; Ding, X.-L.; He, S.-G.; Ge, M.-F. Ground State Structures of $\text{Fe}_2\text{O}_{4-6}^+$ Clusters Probed by Reactions with N_2 . *J. Phys. Chem. A* **2009**, *113*, 5302–5309.
- (37) Frisch, M. J.; Trucks, G. W.; Schlegel, H. B.; Scuseria, G. E.; Robb, M. A.; Cheeseman, J. R.; Scalmani, G.; Barone, V.; Mennucci, B.; Petersson, G. A.; et al. *Gaussian 0901*, Revision A; Gaussian Inc.: Wallingford, CT, 2009.
- (38) Becke, A. D. Density-Functional Thermochemistry. III. The Role of Exact Exchange. *J. Chem. Phys.* **1993**, *98*, 5648–5652.
- (39) Lee, C. T.; Yang, W. T.; Parr, R. G. Development of the Colle-Salvetti Correlation-Energy Formula into a Functional of the Electron Density. *Phys. Rev. B* **1988**, *37*, 785–789.
- (40) Rassolov, V. A.; Pople, J. A.; Ratner, M. A.; Windus, T. L. DFT Studies of Unique Stereoelectronic Effects of Substituents on Divergent Reaction Pathways of Methylene-cyclobutanone Radical Cations. *J. Chem. Phys.* **1998**, *109*, 1223–1229.
- (41) Anderson, A. B.; Hong, S. Y.; Smialek, J. L. Comparison of Bonding in First Transition-Metal Series: Diatomic and Bulk Sulfides and Oxides. *J. Phys. Chem.* **1987**, *91*, 4250–4254.
- (42) Stephens, P. J.; Devlin, F. J.; Chabalowski, C. F.; Frisch, M. J. Ab Initio Calculation of Vibrational Absorption and Circular Dichroism Spectra Using Density Functional Force Fields. *J. Phys. Chem.* **1994**, *98*, 11623–11627.
- (43) Fowler, W. B. *Physics of Color Centers*; Academic Ed.: New York, 1968.
- (44) Seitz, F. Color Centers in Alkali Halide Crystals. *Rev. Mod. Phys.* **1946**, *18*, 384–408.
- (45) Landman, U.; Scharf, D.; Jortner, J. Electron Localization in Alkali-Halide Clusters. *Phys. Rev. Lett.* **1985**, *54*, 1860–1863.
- (46) Scharf, D.; Jortner, J.; Landman, U. Cluster Isomerization Induced by Electron Attachment. *J. Chem. Phys.* **1987**, *87*, 2716–2723.
- (47) Sunil, K. K.; Jordan, K. D. Negative Ion Formation in Alkali Halide Clusters. *J. Phys. Chem.* **1987**, *91*, 1710–1711.
- (48) Barnett, R. N.; Landman, U.; Scharf, D.; Jortner, J. Surface and Internal Excess Electron States in Molecular Clusters. *Acc. Chem. Res.* **1989**, *22*, 350–357.
- (49) Campana, J. E.; Barlak, T. M.; Colton, R. J.; DeCorpo, J. J.; Wyatt, J. R.; Dunlap, B. I. Effect of Cluster Surface Energies on Secondary-Ion-Intensity Distributions from Ionic Crystals. *Phys. Rev. Lett.* **1981**, *47*, 1046–1049.
- (50) Ma, J.-B.; Xu, B.; Meng, J.-H.; Wu, X.-N.; Ding, X.-L.; Li, X.-N.; He, S.-G. Reactivity of Atomic Hydrogen Radical Anions Bound to Titania and Zirconia Nanoparticles in the Gas Phase: Low-Temperature Oxidation of Carbon Monoxide. *J. Am. Chem. Soc.* **2013**, *135*, 2991–2998.
- (51) Li, X.-N.; Xu, B.; Ding, X.-L.; He, S.-G. Interaction of Vanadium Oxide Cluster Anions with Water: An Experimental and Theoretical Study on Reactivity and Mechanism. *Dalton Trans.* **2012**, *41*, 5562–5570.
- (52) Tian, L.-H.; Zhao, Y.-X.; Wu, X.-N.; Ding, X.-L.; He, S.-G.; Ma, T.-M. Structures and Reactivity of Oxygen-Rich Scandium Oxide Cluster Anions (ScO_{3-5}^-). *ChemPhysChem* **2012**, *13*, 1282–1288.
- (53) Nolan, P. D.; Wheeler, M. C.; Davis, J. E.; Mullins, C. B. Mechanisms of Initial Dissociative Chemisorption of Oxygen on Transition-Metal Surfaces. *Acc. Chem. Res.* **1998**, *31*, 798–804.
- (54) Ding, X.-L.; Wu, X.-N.; Zhao, Y.-X.; He, S.-G. C-H Bond Activation by Oxygen-Centered Radicals over Atomic Clusters. *Acc. Chem. Res.* **2012**, *45*, 382–390.
- (55) Armentrout, P. B.; Loh, S. K.; Ervin, K. M. Transition-Metal Cluster Chemistry: Reactions of Mn_2^+ with O_2 . *J. Am. Chem. Soc.* **1984**, *106*, 1161–1163.

(56) Roach, P. J.; Woodward, W. H.; Castleman, A. W., Jr.; Reber, A. C.; Khanna, S. N. Complementary Active Sites Cause Size-Selective Reactivity of Aluminum Cluster Anions with Water. *Science* **2009**, 323, 492–495.

(57) Reber, A. C.; Khanna, S. N.; Roach, P. J.; Woodward, W. H.; Castleman, A. W., Jr. Reactivity of Aluminum Cluster Anions with Water: Origins of Reactivity and Mechanisms for H₂ Release. *J. Phys. Chem. A* **2010**, 114, 6071–6081.